Journal of Materials Science: Materials in Engineering

ORIGINAL PAPER Open Access

Lifetime assessment of semi-submersible wind turbines by Gaidai risk evaluation method

Oleg Gaidai[1], Alia Ashraf[1], Yu Cao[1*], Jinlu Sheng[2], Yan Zhu[3] and Zirui Liu[1]

Abstract

As the global agenda turns more towards the so-called challenge of climate change and lowering carbon emissions, research into green, renewable energy sources becoming nowadays more and more popular. Offshore wind power, produced by FOWTs (i.e., Floating Offshore Wind Turbines), is one such substitute. It is a significant industrial part of the contemporary offshore wind energy industry and produces clean, renewable electricity. Accurate operational lifetime assessment for FOWTs is an important technical safety issue, as environmental in situ loads can lead to fatigue damage as well as extreme structural dynamics, which can cause structural damage. In this study, in situ environmental hydro and aerodynamic environmental loads, that act on FOWT, given actual local sea conditions have been numerically assessed, using the FAST coupled nonlinear aero-hydro-servo-elastic software package. FAST combines aerodynamics and hydrodynamics models for FOWTs, control and electrical system dynamics models, along with structural dynamics models, enabling coupled nonlinear MC simulation in the real time. The FAST software tool enables analysis of a range of FOWT configurations, including 2- or 3-bladed horizontal-axis rotor, pitch and stall regulation, rigid and teetering hub, upwind and downwind rotors. FAST relies on advanced engineering models—derived from the fundamental laws, however with appropriate assumptions and simplifications, supplemented where applicable with experimental data. Recently developed Gaidai reliability lifetime assessment method, being well suitable for risks evaluation of a variety of sustainable energy systems, experiencing nonlinear, potentially extreme in situ environmental loads, throughout their designed service life. The main advantage of the advocated Gaidai risks evaluation methodology being its ability to tackle simultaneously a large number of dynamic systems' degrees of freedom, corresponding to the system's critical components.

Keywords Floating wind turbine, Reliability, Green energy, Wind energy, Dynamic system

Introduction

One of the most important ecologically friendly renewable green energy sources, that might meet the world's growing energy demands is wind energy. To capture wind energy and produce electricity, offshore WT farms are being built on a regular basis. These wind farms are usually constructed on the continental shelf. Since windspeeds offshore being often higher, than those on land, the offshore wind power sector plays a major industrial role in the electricity supply. Greater in situ windspeeds are often the result of a relatively smooth sea surface. The effective production of renewable energy is dependent on the latest enhancements to the FOWT's modern design. Due to FOWTs' innate vulnerability to ambient wind turbulence and nonlinear aerodynamic and hydrodynamic loads, their extreme dynamics characteristics should be accounted for in both initial design and operations.

There are typically 2 distinct approaches for calculating the design loads of WTs (i.e., Wind Turbine): (a) simulating rare, high-load-level occurrence, e.g., 10,000-year

*Correspondence:
Yu Cao
y_cao@shou.edu.cn
[1] Shanghai Ocean University, Shanghai, China
[2] Chongqing Jiao Tong University, Chongqing, China
[3] Jiangsu University of Science and Technology, Zhenjiang, China

wave; (b) simulating WT reaction under usual operating conditions, then extrapolating joint PDF (i.e., Probability Density Function) of WT failure probability (International Energy Agency, 2020; Poujol et al. 2020; Ferraz de Paula and Carmo 2022; Maienza et al. 2022). For life cycle assessment under environmental impacts for FOWTs in deep-sea areas, see (Brussa et al. 2023). IEC (i.e., International Electrotechnical Commission) 61,400–1 standard, (GWEC 2021) recommends using both techniques to assess characteristic design loads. FOWT in offshore operations has been illustrated in Fig. 1. This study contributes to the 2nd approach (b), (Chen et al. 2022) , by advocating state-of-art methodology, which has already been shown successful for a wide range of naval and marine structures, including FOWTs, offshore platforms, and vessels. The internal bending moments and anchor tensions of the FOWT were numerically calculated to evaluate the reaction of the structural dynamic system. NREL (i.e., National Renewable Energy Laboratory, USA) created the FAST code, a potent nonlinear aero-hydro-servo-elastic modelling toolbox. Modal dynamics is incorporated into the FAST software package to simulate multibody structural dynamics, (Jonkman and Buhl 2005; NOAA 2023; IEC 2009; Haid et al. 2013; Jain et al. 2012). To examine critical FOWT's bending moments and anchor stresses, load data from 2550× 10-min FAST simulations, which spanned about 18 days in total, were assessed. These simulations represented a range of potential in situ meteorological circumstances. Since the 10-min single simulation duration mandated by current regulations for both land-based and offshore-based turbines may not be adequate for combined wind and wave loads on FOWT, extensive numerical Monte Carlo (MC) simulations have been carried out.

Developing more accurate tools to assess critical structural stresses that FOWTs could encounter when operating in choppy waters was the aim of numerous recent studies. (Ronold et al. 1999; Ronold and Larsen 2000; Manuel et al. 2001; Fitzwater and Cornell 2002; Moriarty et al. 2002; Agarwal and Manuel 2008; Barreto et al. 2022; McCluskey et al. 2021). In (Fogle et al. 2008), authors have utilized block maxima extrapolation, to assess critical structural loads. In (Ernst and Seume 2012) authors have accounted for ambient turbulence intensity, while performing a WT risks evaluation study. MC method has been widely utilized by various authors in (Freudenreich and Argyriadis 2007; Gaidai 2022; Peeringa 2009; Abdallah 2015) to assess long-term FOWT fatigue loadings. For predictions of design WT loads, based on limited datasets, see e.g., (Stewart et al. 2015). The techniques described above fit an Extreme Value Distribution, or EVD, to the underlying dataset; nevertheless,

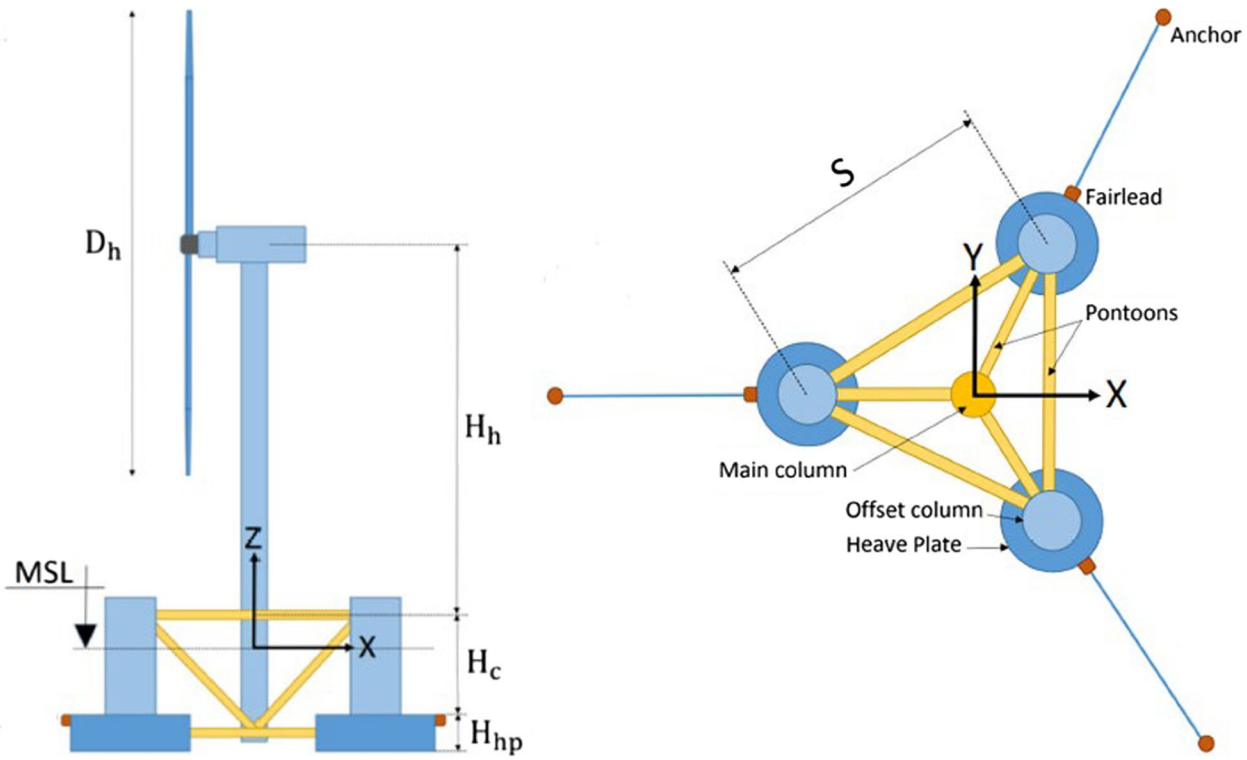

Fig. 1 Example of the Deep-C-wind semi-submersible-type FOWT, (Xu et al. 2022)

this may not meet the asymptotic condition. The latter becomes a crucial matter since it raises the possibility of less conservative outcomes when evaluating design/characteristic values. To allow improved FOWT design and its control system, it is imperative to examine non-linear extreme structural dynamics using more accurate and efficient risks evaluation models and numerical approaches. With improved WT design, extreme climatic loadings will be less likely to cause mechanical damage to FOWTs; precise design load predictions would also enable more efficient sizing of important FOWT components, (Gaidai et al. 2022).

Contemporary risks evaluation approaches that are currently in use in offshore and wind engineering, suggest that modern structural risks evaluation methods are not well-suited to handle high-dimensional dynamic systems, particularly when there are intricate non-linear cross-correlations between the FOWT system's essential components. Primary purpose and objective of the current study was to fill the later research gap, in particular what regards systems high-dimensionality. The operational lifespan evaluation of complex dynamic systems, which is crucial for the robust and long-lasting design of a variety of offshore structures exposed to in situ environmental pressures, is carried out in this study by employing a novel Gaidai risks evaluation methodology. For recent studies on WT safety and reliability, see (Cuesta 2024; Sharar and Hoover 2024; Kenworthy, et al. 2024). In the following Sect. 2 to introduce WT system, Sect. 3 to outline novel reliability methodology, Sect. 4 to report results and numerical findings.

System's description

Obtaining excellent, high-resolution met-ocean data may be challenging. The NOAA (i.e., National Oceanic and Atmospheric Administration, USA) provided the dataset that was utilized in this investigation. Extensive network of floating data collecting buoys being kept up to date by NOAA in both domestic and foreign waters. The NOAA Data Buoy Center offers online access to data from these buoys, (NOAA 2023). Wind directions and observed windspeeds for the specific dataset under analysis in this study have been averaged across 8-min intervals. Significant wave heights may be identified based on 20-min measurements periods. Throughout each 20-min wave measurement interval, the peak-spectral period, along with the wave period with the highest wave energy had been assessed. The measuring buoy station at Cape Elizabeth, located 45 nautical miles northwest of Aberdeen, state of Washington, close to the US continental shelf line, has been selected for this investigation. Combined wind-wave statistics for the indicated site have been produced using hourly historical met-ocean in situ measurements from2010 to 2017. For an MC-based statistical long-term analysis flowchart see Fig. 2. Authors will further refer to all scatter diagram's environmental in situ sea/ocean conditions, including local windspeeds, as "sea states".

Windspeeds should then be extrapolated to a standard FOWT's hub height of 90 m. Anemometers have been installed at Cape Elizabeth buoy, five meters above MSL (i.e., Mean Sea Level). PL (i.e., Power Law) wind shear equation to be utilized

$$U(z) = U(z_r)\left(\frac{z}{z_r}\right)^{\alpha} \tag{1}$$

with α being PL constant, $U(z)$, $U(z_r)$ being windspeed at height z and reference windspeed at elevation z_r, respectively. In this study, PL constant, specified by Eq. (2) has been fixed to α= 0.14, (IEC 2009). The following notations have been employed.

Windspeed U
Significant wave height H_s
Peak spectral wave period T_{p}

In this work, an empirical multi-dimensional joint PDF was formed from the observed buoy dataset through post-processing using only in-situ scatter diagrams, without any assumptions or simplifications. Joint 3D (i.e., 3-Dimensional) PDF $p\left(U, H_s T_p\right)$ in-situ scatter diagrams have been straightforwardly derived from underlying

Fig. 2 Long-term MC-based reliability flowchart

Table 1 Main dimensions of semi-submersible-type FOWT platform

Items	Values
Platform's draft	20.0 m
Spacing between FOWT offset columns	50.0 m
Length of upper FOWT columns	26.0 m
Length of FOWT base columns	6.0 m
Main FOWT column diameter	6.5 m
Upper offset column diameter	12.0 m
FOWT base column diameter	24.0 m
Platform's mass	$1.3{\cdot}10^7$ kg
Platform roll inertia, about CM	$6.8{\cdot}10^9$ kg·m^2
Platform pitch inertia, about CM	$6.8{\cdot}10^9$ kg·m^2
Platform yaw inertia, about CM	$1.2{\cdot}10^{10}$ kg·m^2

Table 2 5-MW FOWT properties

Items	Values
Rotor's orientation	Up-wind
Cut-in/Rated/Cut-off windspeeds	3 m/s, 11 m/s, 25 m/s
Rotor's mass	110 kg
Nacelle's mass	240 kg
Tower's mass	348 kg
Hub's height	90 m

in-situ met-ocean dataset. In the FAST numerical simulation, 3D PDF $\left(U, H_s T_p\right)$ has been used as an input; wind/wave misalignments have not been accounted for. Gaidai risks evaluation approach being particularly efficient for high-dimensional PDFs. In the next, predictions, obtained from a direct MC-based long-term numerical simulation approach, will be compared with those by the Gaidai risks evaluation method. The direct MC-based approach is schematically displayed in Fig. 2. The OC4 semi-submersible Deep-C-wind floating dynamic system, supporting the FOWT platform, has been selected in this study. Three external offset columns and one central main column make up the semi-submersible type FOWT platform. The FOWT bottom has heave plates affixed to it to lessen excessive heave motions. Table 1 displays the principal dimensions of the semi-submersible type FOWT platform under examination.

NREL 5-MW baseline FOWT had been mounted on top of the Deep-C-wind semi-submersible-type FOWT platform. Hub's height of the FOWT cylindrical tower was 90 m, 126 m for the FOWT 3-bladed rotor. The 5-MW FOWT baseline's summary properties have been presented in Table 2.

FOWT structural dynamics, as well as applied aerodynamic and gravitational stresses, have been modelled using FAST and Aero-Dyn. The FOWT dynamics encompass tower elasticity and dynamic interaction between the FOWT platform and tower movements. FAST utilizes a numerical model that combines modal dynamics along with structural dynamics for multibody dynamics, (Jonkman and Buhl 2005).

All relevant/key FOWT system's DOFs (Degrees Of Freedom) have been well accounted for in FAST numerical simulation, including 2 flap-wise and 1 edge-wise moment, 1 torsion DOF for FOWT powertrain, 1 variable generator-speed DOF for FOWT nacelle. The FOWT platform had 3 DOFs for translation (surge, sway, heave), 3 for rotation (roll, pitch, yaw), 2 fore-aft and 2 side-to-side FOWT tower modes DOFs. To numerically simulate the FOWT dynamic system's cross-correlated key/critical components, the aero-hydro-servo-elastic simulation software package FAST, (Jonkman and Buhl 2005) has been utilized. Turb-Sim software has been utilised to generate stochastic wind speed fields on a 145 m wide, 31× 31 square grid. When modelling aerodynamics of baseline WTs, the Aero-Dyn module of the FAST code, which utilizes the BEM (i.e., Blade Element Momentum) technique, in order to describe FOWT aerodynamics, takes into consideration FOWT rotor wake effects, in addition to dynamic stall. To model FOWT hydrodynamic loads, the FAST's Hydro-Dyn module had been utilized, combining potential flow equations for large diameter structure, given Morison's hydrodynamic force equation $F_D = \frac{1}{2} C_D \rho A v^2$ for offshore slender structure, with C_D being drag coefficient, ρ being water density, A tubular cross-sectional area, $v$being water particle velocity. Morison's equation effectively takes into account the viscous drag external loads operating on FOWT via the drag force component. FAST numerical models have done a good job of accounting for second-order hydrodynamic forces. Standard IEC-61400–1 states that to assess ultimate loads over 50 years, based on standard IEC-61400–3, at least 15 short-term MC simulations, 10 min duration each, are required, (IEC 2009). Note the latter 10-min MC sample's duration being typical for FOWT aerodynamic modelling, as opposed to 3-h direct MC runs for the hydrodynamic type of problems, involving 3-h stationary sea/ocean states. Figure 3 presents a time-series example for the FOWT tower's fore-aft bending moment, affecting the FOWT tower's base.

Extensive experimental effort of FOWT modelling methodologies being required to give experimental data that is essential in verifying the completion of OC4, OC5, and similar projects. The OC5 FAST numerical data, the experimental/lab findings, and the numerical results all showed an average underprediction of the FOWT tower top ultimate shear loads, tower-base loads, and upwind mooring/hawser tensions of around 10%, 14%, 20%,

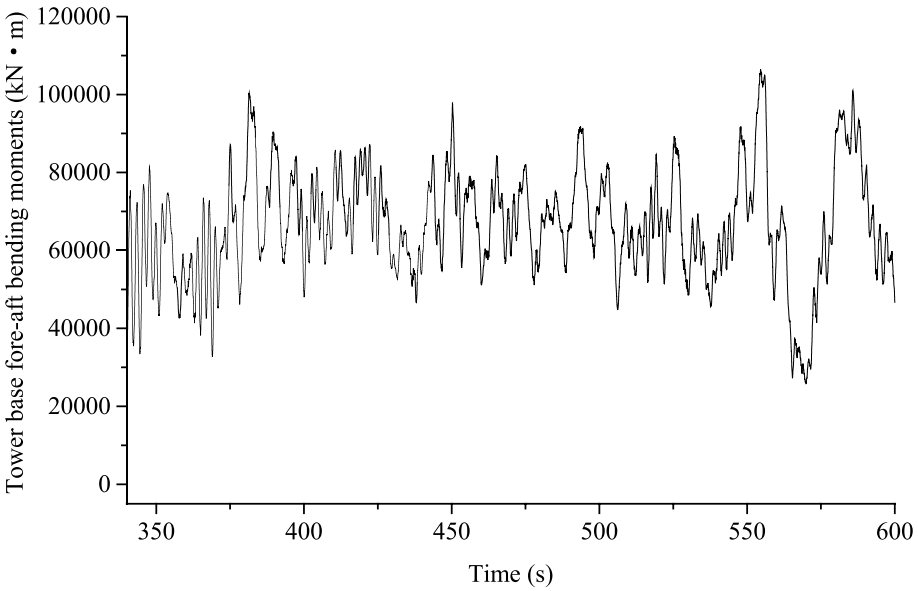

Fig. 3 FOWT tower base's fore-aft bending moment timeseries, $U_{hub} = 11$m/s, (Xu et al. 2022)

respectively, (Robertson et al. 2017). The authors relied on FAST as an accurate numerical simulation tool, based on the latter experimental validation findings.

Gaidai risks evaluation method

LTD (i.e., Life Time Distribution) estimation approach for complex, nonstationary, nonlinear FOWT dynamic systems, subjected to various risk/hazard modes over specified service timelapse, is briefly discussed in this section. FOWT dynamic system successive lifetimes L_i, $i = 1,2,\ldots$, measured in-between consecutive failure/hazard/risk/damage threshold crossings, generating sequential L values. The lifetime of the FOWT dynamic system is thus represented by L, which is a random variable. LTD of complex nonstationary FOWT systems cannot be easily calculated, using current technical risks evaluation methodologies, particularly when there are many important dimensions and components (failure/hazard modes) in the system. It is now possible to evaluate the target CDF (i.e., Cumulative Distribution Function)

$$\mathrm{LDT}(L) \equiv \mathrm{Prob}(\mathrm{Lifetime} \le L) \tag{2}$$

using extensive direct type MC simulations, or sufficient measurement data, if available for the FOWT dynamic system, (Gaidai et al. 2022; Gaidai et al. 2022; Gaidai et al. 2022; Gaidai 2022; Gaidai et al. 2022; Gaidai and Xing 2022; Gaidai et al. 2022). The expense of computational resources and lab testing may frequently be prohibitive for the majority of complex dynamic energy/environmental systems. The authors of this study advocate a novel LTD assessment methodology for FOWT systems that lowers the cost of computation and measurement during the FOWT system's design phase, Fig. 4.

Consider the vector $(X(t), Y(t), Z(t), \ldots)$, which represents the MDOF (Multi-Degree Of Freedom) system's overall dynamic that has been either simulated or measured within a representative timelapse $(0, T)$. This vector is made up of the key/critical components/dimensions of the FOWT system, which are inter-correlated nonlinear FOWT system's critical components (loads or responses The 1D (1-Dimensional) critical/key global maxima of the FOWT system are represented by the notations $X_T^{max} = X(t)$, $Y_T^{max} = Y(t)$, $Z_T^{max} = Z(t), \ldots$ The authors define "representative" timelapse $(0, T)$ as a big enough value of T in relation to the autocorrelation of the dynamic FOWT system and the relaxation temporal scales.

The crucial process $X = X(t)$ a dynamic system has local maxima $X_1, \ldots, X_{N_X}$ that happen at discrete, temporally increasing instants $t_1^X < \cdots < t_{N_X}^X$ inside $(0, T)$. For additional MDOF crucial components, such as $Y(t), Z(t)$, and others, specifically $Y_1, \ldots, Y_{N_Y}; Z_1, \ldots, Z_{N_Z}$ similar definitions must be used. For the purpose of simplicity, all local maxima for the critical elements of the FOWT system have been assumed to be positive.

Next,

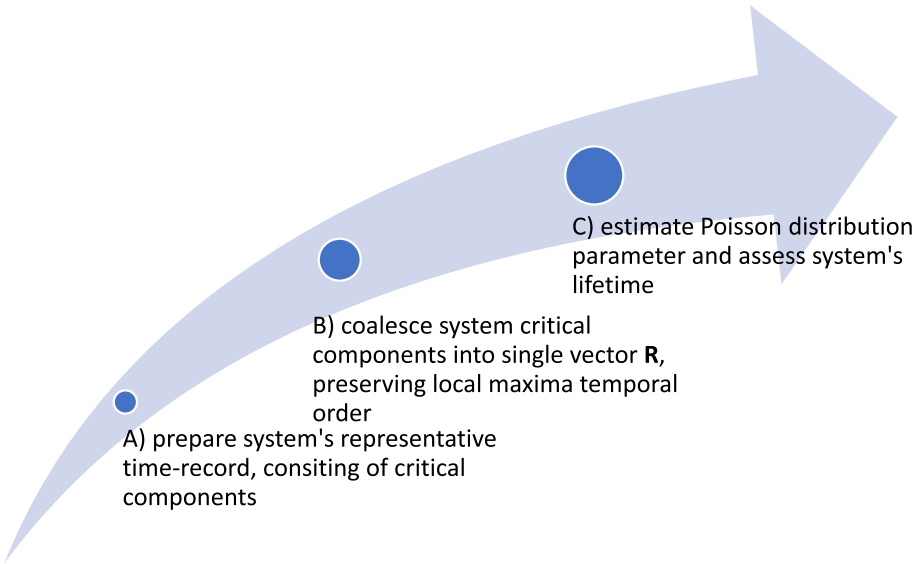

Fig. 4 Gaidai risks evaluation methodology's flowchart

$$P = \iiint_{(0,0,0,\dots)}^{(\eta_X,\eta_Y,\eta_Z,\dots)} p_{X_T^{\max},Y_T^{\max},Z_T^{\max},\dots}\left(x_T^{\max}, y_T^{\max}, z_T^{\max}, \dots\right) dx_T^{\max} dy_T^{\max} dz_T^{\max} \dots \tag{3}$$

being the target probability of the dynamic system survival, andη_X,η_Y,η_Z,... being the critical/hazard/limit values of the FOWT system's component parts; $p_{X_T^{max},Y_T^{max},Z_T^{max},\dots}$ being the system's joint PDF of each global maxima of the system's component parts. It could not be practically possible to predict directly the joint PDF$p_{X_T^{max},Y_T^{max},Z_T^{max},\dots}$, and therefore the FOWT system's goal survival chances/probability P if the dynamic FOWT system's NDOF (number of degrees of freedom) is enormous. Based on the underlying system's lifespan CDF distribution$LTD(L)$, provided by Eq. (1), it is simple to evaluate the hazard/failure risk/probability $P_{failure}$ of the FOWT system as well as the associated system's expected lifetime L_{expected}

$$\frac{T}{P_{\text{failure}}} = L_{\text{expected}} \equiv E[L] = \int_0^{\infty} L d\text{LTD}(L) \tag{4}$$

having the likelihood, risk, and failure of the system$P_{\text{failure}} = 1 - P$, which is supplementary to the survival probability of the FOWT system$P$. If any of the 1D (unidimensional) critical components of the dynamic FWT system $X(t)$ exceedingη_X, $Y(t)$ surpassingη_Y, $Z(t)$ exceedingη_Z, etc.—are exceeded, the system is said to have failed (or been damaged). Individually defined fixed failure, danger, and damage levels $(X, Y, Z, \dots$ etc.) for each system's 1D critical and crucial components$X_{N_X}^{max} = \{X_j ; j = 1, \dots, N_X\} = X_T^{max}$, $Y_{N_Y}^{max} = \{Y_j ; j = 1, \dots, N_Y\} = Y_T^{max}$,$Z_{N_z}^{max} = \{Z_j ; j = 1, \dots, N_Z\} = Z_T^{max}$, ... 1D key components of a dynamic system, X, Y, Z,... being rescaled, and then non-dimensionalized

$$X \to \frac{X}{\eta_X}, Y \to \frac{Y}{\eta_Y}, Z \to \frac{X}{\eta_Z}, \dots \tag{5}$$

resulting in the crucial components of the dynamic FOWT system being non-dimensional, with target failure probability $P = P(1)$ and target hazard/failure/risk/damage limits $\lambda = 1$. $P(\lambda)$ is a non-dimensional level λ smooth C^1 function. The 1D critical components local maxima of the dynamic FOWT system are merged into a single temporally increasing vector $\boldsymbol{R}(t) \equiv \overrightarrow{R} = (R_1, R_2, \dots, R_N)$ in accordance with the corresponding temporal vector of the merged FOWT system $t_1 < \dots < t_N, N \le N_X + N_Y + N_Z + \dots$. Every local maxima of R_j came into contact with the local maxima of the dynamic FOWT system critical component, which corresponded $X(t)$ or $Y(t)$, or $Z(t)$, or other dynamic system components, (Gaidai et al. 2022; Gaidai et al. 2022; Gaidai et al. 2022). For constructed synthetic $\overrightarrow{R}$-vector thus having no data loss, see Fig. 5. In simple words, the $\overrightarrow{R}$ vector has been obtained by the temporal coalescing

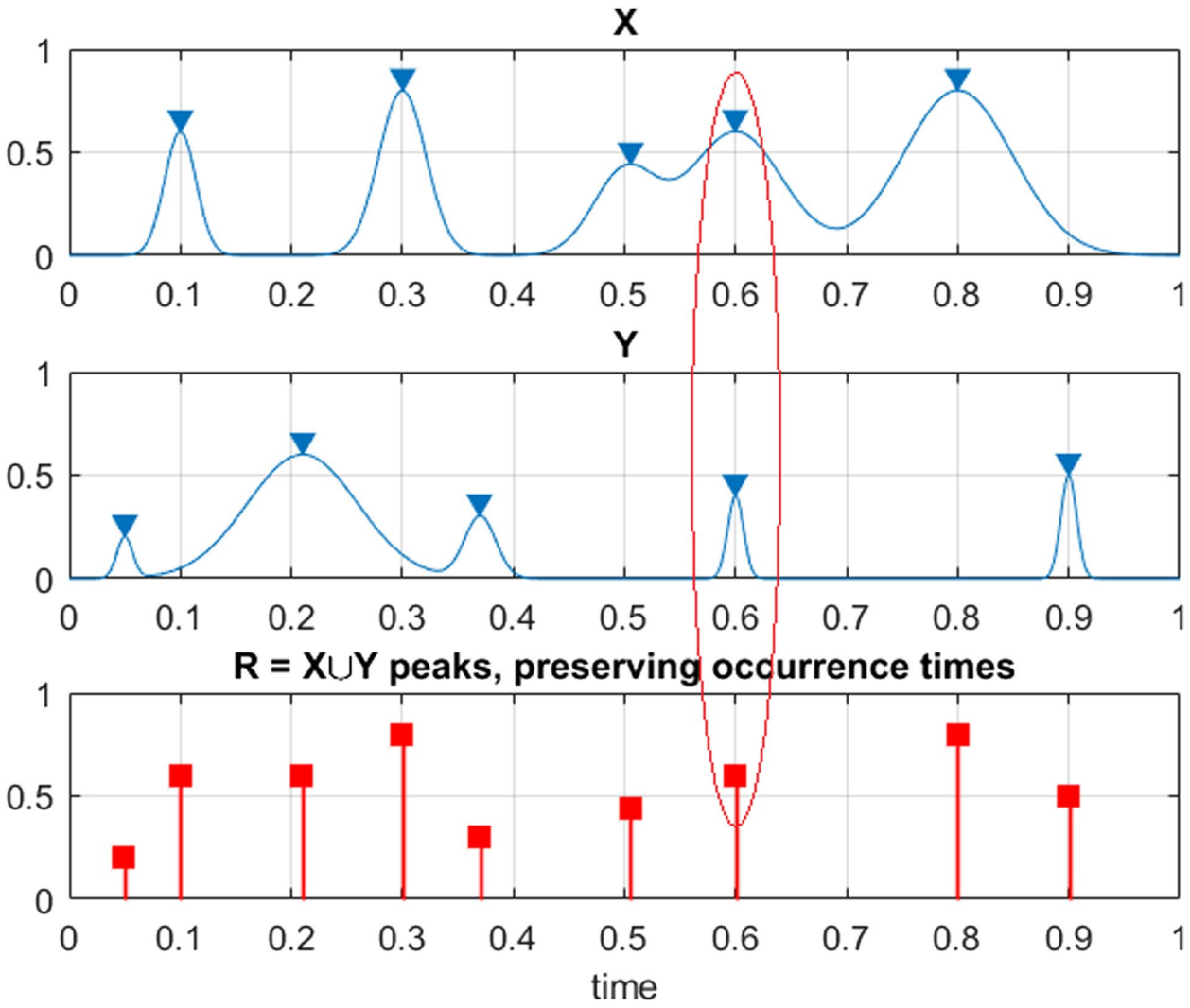

Fig. 5 Example of how 2 components, X, Y being merged into 1 new synthetic vector $\overrightarrow{R}$. Red ellipse highlights the case of simultaneous maxima for different system's components. Nondimensional parameter λ on the vertical axis

of all system component's local maxima. The advocated method applies to any FOWT system's cross-correlation pattern. If two different systems' critical components have temporally coincided local maxima, then only their single maximum is taken into account, see Fig. 5, red ellipse. Also, inequality $N \leq N_X + N_Y + N_Z + ...$ indicates the same issue. In the case of clustering of neighbouring local maxima, the de-clustering procedure has to be done. The non-exceedance (system's survival) probability $P(\lambda)$ must be reevaluated for $k < j \leq N$ (level of conditioning k) in order to eliminate clustering between the local maxima of the temporally neighbouring system's components. The approximation that was first proposed by Eq. (6) may now be further stated as

$$\begin{aligned} &\text{Prob}\left\{R_j \leq \eta_j^{\lambda} | R_{j-1} \leq \eta_{j-1}^{\lambda}, \ldots, R_1 \leq \eta_1^{\lambda}\right\} \approx \\ &\approx \text{Prob}\{R_j \leq \eta_j^{\lambda} | R_{j-1} \leq \eta_{j-1}^{\lambda}, \ldots, R_{j-2} \leq \eta_{j-k}^{\lambda}\} \cdot \text{Prob}(R_1 \leq \eta_1^{\lambda}, \ldots, R_k \leq \eta_k^{\lambda}) \end{aligned} \tag{6}$$

The objective is to maintain a record of every individual damage, danger, and failure that happened locally and originally in time. This will lessen the likelihood of intercorrelated local exceedances and cascade (i.e., de-clustering). Given that the MDOF

FOWT system is thought to be piecewise ergodic, the chance of the system failing or sustaining damage $p_k(\lambda) := Prob\{R_j > \eta_j^{\lambda} | R_{j-1} \le \eta_{j-1}^{\lambda}, R_{j-k+1} \le \eta_{j-k+1}^{\lambda}\}$ for $j \ge k$ is independent of j and only dependent on the degree of conditioning k. Now, the likelihood of non-exceedance may be evaluated as

$$P_k(\lambda) \approx \exp\left(-N \bullet p_k(\lambda)\right), k \ge 1 \tag{7}$$

Note that Eq. (7) follows from Eq. (6) if neglecting $\text{Prob}(R_1 \le \eta_1^{\lambda}, \ldots, R_k \le \eta_k^{\lambda}) \approx 1$, as design failure/damage/hazard probability being of small order of magnitude, with $N \gg k$, (Gaidai et al. 2022; Gaidai et al. 2022; Gaidai et al. 2022). Regarding the conditioning parameter$k$, convergence is required

$$P = \lim_{k\to\infty} P_k(1); p(\lambda) = \lim_{k\to\infty} p_k(\lambda) \tag{8}$$

The synthetic $\overrightarrow{R}$-vector of the built system exhibits a net 0 data loss, (Gaidai et al. 2023; Gaidai et al. 2023; Gaidai et al. 2023; Zhang et al. 2023; Liu et al. 2023; Gaidai et al. 2023). Now that the synthetic vector $\overrightarrow{R}$ has been presented, the stochastic longevity variable L may be defined along with the corresponding temporally increasing occurrence temporal instants $t_1 < \cdots < t_N$

$$L_i = t_i - t_{i-1} \tag{9}$$

where $i = 2, \ldots, N$. The integrated synthetic process $\boldsymbol{R}(t)$ the FOWT system thus contains crucial information about the target LTD PDF. Currently, target FOWT survival chances/probability can be evaluated using the MUR (i.e., Mean Up-crossing Rate) function $P = P(1)$

$$P(\lambda) \approx \exp\left(-\nu^{+}(\lambda)\, T\right), \nu^{+}(\lambda) = \int_0^{\infty} \zeta p_{R\dot{R}}(\lambda, \zeta) d\zeta \tag{10}$$

with $\nu^{+}(\lambda)$ denoting the MUR function of the hazard/failure/risk/damage threshold level λ for the non-dimensional synthetic vector $R(t)$ of the FOWT system as previously discussed, (Liu et al. 2023; Gaidai 2023; Gaidai et al. 2023; Yakimov et al. 2023; Gaidai et al. 2023; Sun et al. 2023; Gaidai et al. 2023; Yakimov et al. 2023). For the MUR function, Rice's formula is represented by Eq. (5), where the joint PDF corresponding to $\left(R, \dot{R}\right)$ is represented by $p_{R\dot{R}}$ and the time-derivative is given by $\dot{R} = R\prime(t)$. The dynamic FOWT system approaches the pre-established threshold of $\lambda \to 1$ for failure, risk, hazard or damage

$$\log_{\lambda\to 1} P_{\text{failure}}(\lambda) = \frac{T}{L_{\text{expected}}}, p(\lambda) \bullet N \approx \nu^{+}(\lambda)\, T \Rightarrow L_{\text{expected}} = \frac{T}{p(1)N} \approx \frac{1}{\nu^{+}(1)} \tag{11}$$

The MDOF dynamic FOWT system had been assumed to be jointly quasi-stationary. A novel short-term environmental, sea, or ocean state is given an in-situ environmental scatter diagram with $m = 1, .., M$ environmental/sea/ocean states, each with its own occurrence probability/chances probability/chances q_m, with $\sum_{m=1}^{M} q_m = 1$, (Gaidai et al. 2023; Gaidai et al. 2023; Gaidai et al. 2023; Gaidai et al. 2023; Sun et al. 2023; Gaidai et al. 2024; Gaidai et al. 2024; Gaidai et al. 2024). Currently, a long-term probability equation indicates that

$$\text{LTD}(L) \equiv \sum_{m=1}^{M} LTD_m(L) q_m \tag{12}$$

Applying analogous functions to Eq. (6) for $p_k(\lambda, m)$, which represent each unique short-term ambient sea/ocean condition/state with number m. The following Section will show how to evaluate the relevant LTD q quantiles.

$$L_q = \text{LTD}^{-1}(q) \tag{13}$$

using underlying time series that are either MC simulated or measured, where $^{\circ}$ denotes functional composition, $q \in (0, 1)$ and LTD^{-1} are the inverse of LTD, and $\text{LTD}^{\circ} LTD^{-1} = 1$ is the identity-operator. The target lifespan distribution will resemble Poisson's distribution with the parameter $\nu^{+}(\lambda)\, T$since the failure, hazard, or damage events of the FOWT dynamic system become almost independent at high failure, hazard, risk, or damage levels. Current study primarily focused on the Poisson-type process, but it may have broader implications if any failure, hazard, risk, or damage of any of the critical components or dimensions of the FOWT system does not indicate that the system is about to collapse, but instead merely consists of a sequence of interdependent local maxima of the FOWT system's critical components, (Gaidai 2024; Gaidai 2024; Gaidai et al. 2024; Gaidai et al. 2024) (Yuan 2023; Gaidai 2022; Gaidai. 2023; Gaidai 2023)

Results

In this section, the efficacy of the previously mentioned Gaidai risks evaluation methodology is illustrated through an analysis of three dynamic key/critical components of the FOWT system using the Gaidai risks evaluation method: 1) the FOWT tower's fore-aft bending moment; 2) the FOWT blade's root's out-of-plane bending moment; and 3) the FOWT anchor's tension.

FOWT dynamics is a difficult dynamic system to assess due to its cross-correlated, multidimensional, highly nonlinear characteristics. Moreover, system risks evaluation research is crucial for FOWTs working in extreme weather conditions. This section will demonstrate the Gaidai risks evaluation technique in practice. 3 FOWT system's critical components X, Y, Z(internal forces in our study's case), defined above, had been selected as an engineering example of a 3D dynamic FOWT system. For each FOWT system's critical component, its failure/hazard/risk limit had been set equal to its recorded global maximum, but increased twice; note that this being a purely subjective choice, done only for an illustration, (Sun et al. 2023; Gaidai et al. 2024; Gaidai et al. 2024; Gaidai et al. 2024; Gaidai 2024; Gaidai 2024; Gaidai et al. 2024. The three recorded time series' local maxima were then integrated into a single synthetic time series, $\overrightarrow{R} = (\{X_1, Y_1, Z_1\}, \ldots, \{X_N, Y_N, Z_N\}, \ldots)$ with the rising periods of occurrences of the local maxima of the three important components of these systems being utilized to sort each set $\{X_j, Y_j, Z_j\}$. As a result, the critical dimensions and components of all three systems become non-dimensional, with the same $\lambda = 1$ hazard, risk, failure, and risk limitations. The non-dimensional constructed synthetic vector $\overrightarrow{R}$ in (Fig. 6a) is derived from assembled local maxima of FOWT critical components (in this case, internal forces), with lower values $\lambda \geq 0$ being irrelevant for target hazard/failure/damage PDF tail's extrapolation towards the target threshold/level $\lambda = 1$. The $\lambda > 0.3$ cut-on limit has been used purely illustratively. Since it has been made up of various FOWT critical components, having distinct measurement units—in our example, Nm for bending moments and kN for forces, the FOWT system's vector $\overrightarrow{R}$ does not possess any particular physical meaning. Figure 6a) presents non-dimensional system's synthetic vector $\overrightarrow{R}$. Figure 6b) presents extrapolation towards a 1-year return period of interest, marked with the red star, along with PDF plot illustrating LTD. CI (i.e., Confidence Intervals) have been estimated empirically based on inverse normal distribution.

In Fig. 6b), the extended 95% CI is highlighted with 2 dotted lines. Due to convergence, about conditioning parameter k, namely $\lim_{k\to\infty} p_k(\lambda) = P(\lambda)$, with conditioning parameter $k = 6$found to be convergent, for further evidence, see (Gaidai et al. 2023). Figure6b) displays a relatively low 95% CI, which is beneficial. As demonstrated in Fig. 6b), (Gaidai et al. 2023), MUR from the equation$P(\lambda) \approx \exp(-\nu^+(\lambda)\, T)$ had been extrapolated in order to attain desired failure/hazard/risk threshold $\lambda = 1$. With the target dynamic FOWT system's failure/risk/hazard/damage rate, expressed in years^{-1}, and an expected FOWT system lifetime of $L_{expected} = \frac{T}{p(\lambda)N}$, according to Eq. (9), it can be concluded that the target dynamic FOWT system's LTD will follow Poisson-type PDF, with temporal parameter $\nu^+(1)$.

Hence, critical factor to assess expected FOWT system's lifetime being the MUR ν^+, presented by Fig. 6b). Note that this is being methodological study, thus not a case study, hence authors did not aim to present exact numbers, diagrams and tables, but rather advocated novel Gaidai risks evaluation methodology, (Gaidai et al. 2023; Yakimov et al. 2023; Gaidai et al. 2023; Sun et al. 2023; Gaidai et al. 2023; Yakimov et al. 2023). Figure6b) presents the PDF tail's extrapolation of 3 decimal orders of magnitude, meaning that the MC-type method's computational costs could be saved by about 10^3 times. With its robust statistical features and relatively simple approach, the Gaidai multivariate risks evaluation methodology appears to be a compelling approach. It often agrees with data-intensive POT (i.e., Peaks Over the Threshold), when examining extended return levels. Although the data's extreme value distribution may be fully represented nonparametrically by the Gaidai multivariate risks evaluation methodology, a specific class of parametric distributions was established in order to facilitate extrapolation to extended return period levels. The Gumbel-type PDF is the suitable asymptotic extreme value distribution in certain instances, which is the focus of this class of PDFs. This assumption is supported in the context of this chapter by the underlying statistics on water level, which always fall inside the zone of attraction of an asymptotic Gumbel-type PDF for the extremes.

Conclusions

Traditional timeseries risks evaluation design methods may not always be able to include complex cross-correlations across various system's critical components, due to system's high-dimensionality. Gaidai multivariate risks evaluation methodology's primary benefit lies within its capacity to assess lifetime distribution of multi-dimensional nonlinear nonstationary dynamic system. Current study investigated FOWT systems' performance, given realistic environmental settings, resulting in accurate assessment of FOWT lifetime distribution. The proposed approach's theoretical underpinnings have been presented in detail. In order to optimally utilize underlying datasets—which can be measured or MC numerically simulated—novel, accurate, dependable approaches have to be further developed. Evaluating structural failure or damage risk, based on direct measurements or extensive MC simulations is not always affordable. Current study's primary goal was to offer a multifunctional, trustworthy, easy-to-use solution for multidimensional offshore energy systems design. The proposed strategy

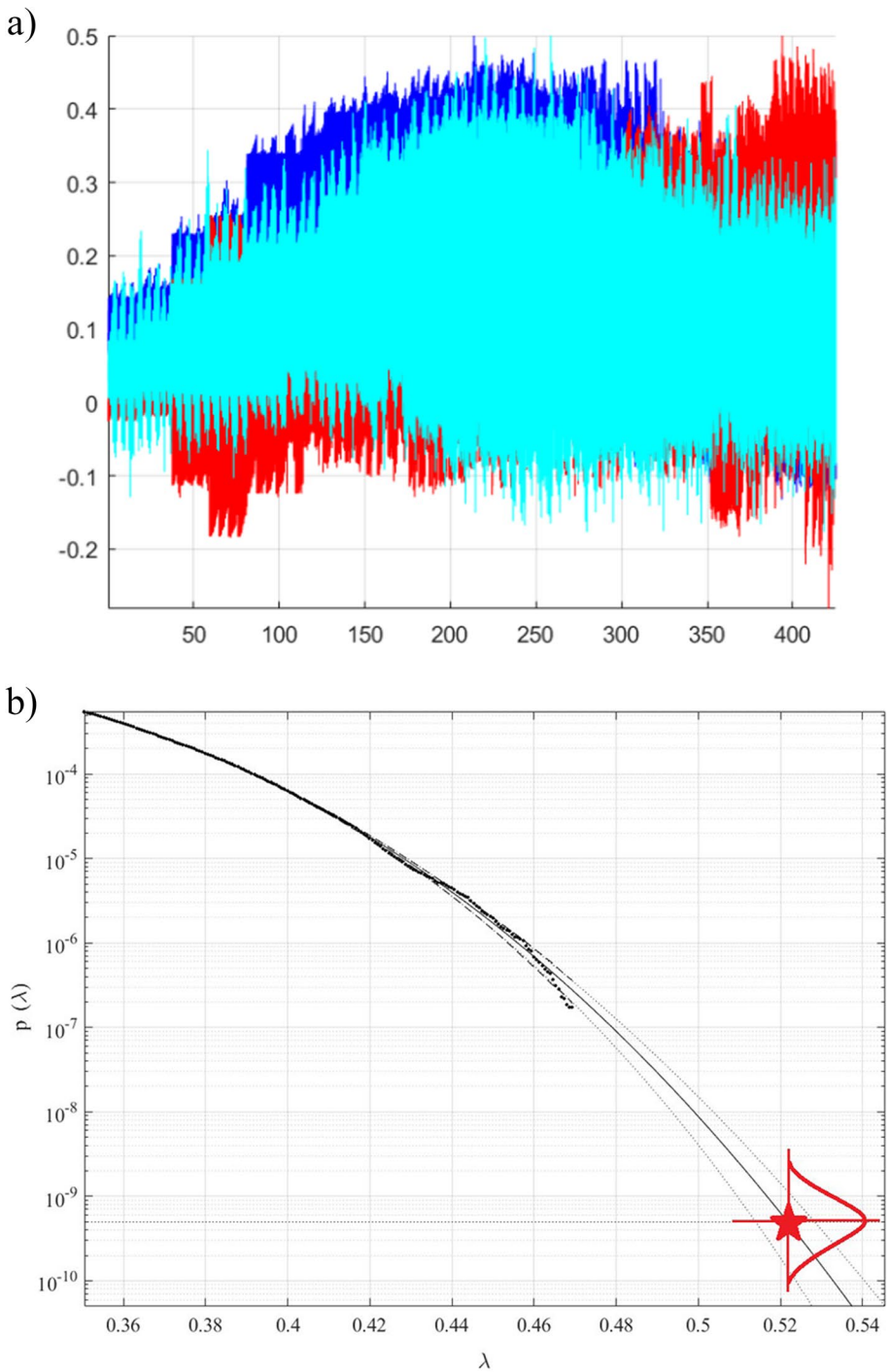

Fig. 6 **a**) Non-dimensional system's vector $\overrightarrow{R}$, index on the x-axis. **b** Extrapolation of $p_k(\lambda)$ towards failure/risk/damage level (star). An extrapolated 95% CI being indicated with 2 dotted lines. Vertical PDF plot illustrates LTD

has produced reasonably narrow confidence intervals; thus, the suggested approach can be helpful for nonlinear dynamic systems design. The examined FOWT example does not in any way limit potential use of the suggested methodology. Primary benefit of the advocated risk assessment methodology being is ability to treat reliability of multidimensional systems with practically unlimited number of dimensions or components. For non-stationary systems, the Gaidai risks evaluation approach can still be applied, utilizing an in-situ scatter

diagram, composed of multiple short-term stationary sea states. In the latter case the underlying trend should be identified first – an example of an underlying trend could be a dynamic system with deterioration, where initial manufacturing faults cause local fractures to gradually grow, e.g., in welded hot spots. Material properties have also to be taken into account.

Acknowledgements
None.

Conflict of interest
Authors declare no conflict of interest.

Authors' contributions
All authors have contributed equally.

Funding
No funding had been received.

Availability of data and materials
Data available on request from the corresponding author.

Declarations

Ethics approval and consent to participate
Not applicable.

Consent for publication
All authors agreed.

Competing interests
No competing interests.

Received: 17 April 2024 Accepted: 29 May 2024
Published online: 22 June 2024

References

Agarwal P, Manuel L (2008) Extreme loads for an offshore wind turbine using statistical extrapolation from limited field data. Wind Energy: Int J Progr Appl Wind Power Conversion Technol 11(6):673–684

Barreto D, Karimirad M, Ortega A (2022) Effects of simulation length and flexible foundation on long-term response extrapolation of a bottom-fixed offshore wind turbine. J Offshore Mechanics Arctic Engine 144(3):032001

Brussa G, Grosso M, Rigamonti L (2023) Life cycle assessment of a floating offshore wind farm in Italy. Sustain Prod Consumpt 39:134–144. https://doi.org/10.1016/j.spc.2023.05.006

Chen Z, Yu J, Sun J, Tan M, Yang S, Ying Y, Qian P, Zhang D, Si Y (2022) Load reduction of semi-submersible floating wind turbines by integrating heaving-type wave energy converters with bang-bang control. Front Energy Res 10:929307. https://doi.org/10.3389/fenrg.2022.929307

Cuesta, J., et al., 2024, "Challenges on prognostics and health management for wind turbine components", J Phys Conf Ser. https://doi.org/10.1088/1742-6596/2745/1/012003

Ernst B, Seume JR (2012) Investigation of site-specific wind field parameters and their effect on loads of offshore wind turbines. Energies 5(10):3835–3855

Ferraz de Paula L, Carmo BS (2022) Environmental Impact assessment and life cycle assessment for a deep water floating offshore wind turbine on the Brazilian continental shelf. Wind 2022(2):495–512. https://doi.org/10.3390/wind2030027

Fitzwater LC, Cornell A (2002) Predicting the long-term distribution of extreme loads from limited duration data: comparing full integration and approximate methods. J Sol Energy Eng 124(4):378–386

Fogle J, Agarwal P, Manuel L (2008) Towards an improved understanding of statistical extrapolation for wind turbine extreme loads. Wind Energy Int J Progr Appl Wind Power Conversion Technol 11(6):613–635

Gaidai O, Cao Y, Xing Y, Balakrishna R (2023) Extreme springing response statistics of a tethered platform by deconvolution. Int J Naval Architect Ocean Engine 15:100515. https://doi.org/10.1016/j.ijnaoe.2023.100515

Gaidai O, Cao Y, Xing Y, Wang J (2023) Piezoelectric energy harvester response statistics. Micromachines 14(2):271. https://doi.org/10.3390/mi14020271

Gaidai O, Cao Y, Xu X, Xing Y (2023) Offloading operation bivariate extreme response statistics for FPSO vessel. Scient Rep 13:4695. https://doi.org/10.1038/s41598-023-31533-8

Gaidai, O., Cheng, Y., Xu, X., Su, Y., 2018, "Long-term offshore Bohai bay Jacket strength assessment based on satellite wave data", Ships and offshore structures, 2018

Gaidai O, Fu S, Xing Y (2022) Novel reliability method for multidimensional nonlinear dynamic systems. Marine Struct 86:103278. https://doi.org/10.1016/j.marstruc.2022.103278

Gaidai, O., Krokstad, J., 2009, "Extreme Response Statistics of Fixed Offshore Structures Subjected to Ringing Loads", OMAE2009-79106; pp. 93-99Abdallah, I., 2015, Assessment of extreme design loads for modern wind turbines using the probabilistic approach, DTU Wind Energy. DTU Wind Energy PhD No. 0048

Gaidai, O., Krokstad, J., 2014, "Extreme Response Statistics of Fixed Offshore Structures Subjected to Ringing Loads", Journal of Offshore Mechanics and Arctic Engineering-Transactions of The ASME 2014 ; Vol. 136 (3)

Gaidai, O., Næss, A., Stansberg, C., 2012, "Airgap statistics for a tension leg platform. 31st International Conference on Ocean, Offshore and Arctic Engineering (OMAE 2012); 2012-07-01 - 2012-07-06

Gaidai, O., Sheng, J., Cao, Y. et al., 2024. "Limit hypersurface state of art Gaidai reliability approach for oil tankers Arctic operational safety. J Ocean Eng Mar Energ https://doi.org/10.1007/s40722-024-00316-2

Gaidai O, Sheng J, Cao Y, Zhang F, Zhu Y, Liu Z (2024c) "Gaidai multivariate risk assessment method for cargo ship dynamics", Urban. Plan Trans Res 12:1. https://doi.org/10.1080/21650020.2024.2327362

Gaidai, O., Storhaug, G., Naess, A., 2016, "Extreme Value Statistics of Large Container Ship Roll", Journal of Ship Research, Vol 60(2), pp. 92-100

Gaidai, O., Storhaug, G., Næss, A., 2019, "Statistics of extreme hydroelastic response for large ships", Marine Structures, Vol 61, pp. 142–154

Gaidai O, Wang F, Wu Y, Xing Y, Medina A, Wang J (2022) "Offshore renewable energy site correlated wind-wave statistics. Probabil Engine Mechan 68:103207. https://doi.org/10.1016/j.probengmech.2022.103207

Gaidai O, Wang F, Yakimov V, Sun J, Balakrishna R (2023) Lifetime assessment for riser systems. Grn Tech Res Sustain 3:4. https://doi.org/10.1007/s44173-023-00013-7

Gaidai O, Wang K, Wang F, Xing Y, Yan P (2022) Cargo ship aft panel stresses prediction by deconvolution. Marine Struct 88:103359. https://doi.org/10.1016/j.marstruc.2022.103359

Gaidai O, Wang F, Cao Y et al (2024a) 4400 TEU cargo ship dynamic analysis by Gaidai reliability method. J Ship Trd 9:1. https://doi.org/10.1186/s41072-023-00159-4

Gaidai O, Wang F, Sun J (2024) Energy harvester reliability study by Gaidai reliability method. Climate Resilience Sustainabil 3:264. https://doi.org/10.1002/cli2.64

Gaidai O, Wu Y, Yegorov I, Alevras P, Wang J, Yurchenko D (2022) Improving performance of a nonlinear absorber applied to a variable length pendulum using surrogate optimization. J Vibrat Contr 30:156. https://doi.org/10.1177/10775463221142663

Gaidai O, Xing Y (2022) Novel reliability method validation for offshore structural dynamic response. Ocean Engine 266(5):113016. https://doi.org/10.1016/j.oceaneng.2022.113016

Gaidai O, Xing Y, Balakrishna R (2022) Improving extreme response prediction of a subsea shuttle tanker hovering in ocean current using an alternative highly correlated response signal. Results Engine 15:100593. https://doi.org/10.1016/j.rineng.2022.100593

Gaidai O, Xing Y, Balakrishna R, Xu J (2023) Improving extreme offshore wind-speed prediction by using deconvolution. Heliyon 9:e13533. https://doi.org/10.1016/j.heliyon.2023.e13533

Gaidai O, Xing Y, Xu X (2023) Novel methods for coupled prediction of extreme windspeeds and wave heights. Scient Rep 13:1119. https://doi.org/10.1038/s41598-023-28136-8

Gaidai O, Xing Y, Xu J, Balakrishna R (2023) Gaidai-Xing reliability method validation for 10-MW floating wind turbines. Scient Rep 13(1):8691. https://doi.org/10.1038/s41598-023-33699-7
Gaidai, O., Xu, J., Hu, Q., Xing, Y., Zhang, F., 2022; "Offshore tethered platform springing response statistics"; Scientific Reports, Vol. 12, www.nature.com/articles/s41598-022-25806-x
Gaidai O, Xu J, Xing Y, Hu Q, Storhaug G, Xu X, Sun J (2022) Cargo vessel coupled deck panel stresses reliability study. Ocean Engine 268:113318. https://doi.org/10.1016/j.oceaneng.2022.113318
Gaidai O, Xu X, Xing Y (2023) Novel deconvolution method for extreme FPSO vessel hawser tensions during offloading operations. Results Engine 17:100828. https://doi.org/10.1016/j.rineng.2022.100828
Gaidai O, Xu J, Yan P, Xing Y, Zhang F, Wu Y (2022) Novel methods for wind-speeds prediction across multiple locations. Scient Rep 12:19614. https://doi.org/10.1038/s41598-022-24061-4
Gaidai O, Xu J, Yan P et al (2023) Novel methods for reliability study of multi-dimensional non-linear dynamic systems. Sci Rep 13:3817. https://doi.org/10.1038/s41598-023-30704-x
Gaidai O, Xu J, Yakimov V, Wang F (2023c) Analytical and computational modeling for multi-degree of freedom systems: estimating the likelihood of an FOWT structural failure. J Marine Sci Engine 11(6):1237. https://doi.org/10.3390/jmse11061237
Gaidai O, Xu J, Yakimov V, Wang F (2023) Liquid carbon storage tanker disaster resilience. Environ Syst Decis 43:746. https://doi.org/10.1007/s10669-023-09922-1
Gaidai O, Yakimov V, Wang F, Hu Q, Storhaug G (2023) Lifetime assessment for container vessels. Appl Ocean Res 139:103708. https://doi.org/10.1016/j.apor.2023.103708
Gaidai O, Yakimov V, Wang F, Zhang F, Balakrishna R (2023) Floating wind turbines structural details fatigue life assessment. Scient Rep 13(1):16312. https://doi.org/10.1038/s41598-023-43554-4
Gaidai O, Yakimov V, Wang F, Zhang F (2023) Safety design study for energy harvesters. Sustain Energy Res 10(1):15. https://doi.org/10.1186/s40807-023-00085-w
Gaidai O, Yakimov V, Wang F, Sun J, Wang K (2024) Bivariate reliability analysis for floating wind turbines. Int J Low-Carbon Technol 19:55–64. https://doi.org/10.1093/ijlct/ctad108
Gaidai, O., Yakimov, V., Wang, F. et al., 2024, "Gaidai Multivariate Reliability Method for Energy Harvester Operational Safety, Given Manufacturing Imperfections", Int. J. Precis. Eng. Manuf https://doi.org/10.1007/s12541-024-00977-x
Gaidai O, Yan P, Xing Y (2022) Prediction of extreme cargo ship panel stresses by using deconvolution. Front Mech Eng 8:992177. https://doi.org/10.3389/fmech.2022.992177
Gaidai O, Yan P, Xing Y (2022) A novel method for prediction of extreme wind-speeds across parts of Southern Norway. Front Environ Sci 10:997216. https://doi.org/10.3389/fenvs.2022.997216
Gaidai, O., Yan, P., Xing, Y., Xu, J., Zhang, F., Wu, Y., 2023. "Cargo vessel under ice loadings"; Scientific Reports 13(1), https://doi.org/10.1038/s41598-023-34606-w
Gaidai O, Yurchenko D, Ye R, Xu X, Wang J (2022) Offshore crane non-linear stochastic response: novel design and extreme response by a path integration, Ships and Offshore Structures 17(6):1294–1300
Gaidai O, Yurchenko D, Ye R, Xu X, Wang J (2021) Offshore crane non-linear stochastic response: novel design and extreme response by a path integration. Ships and Offshore Structures 17(6):1294-1300
GWEC, 2021; "Global Wind Report 2021 | GWEC**";** Global Wind Energy Council, 75, http://www.gwec.net/global-figures/wind-energy-global-status/
Hui, G., Gaidai, O., Næss, A., Storhaug, G., Xu, X., 2019, "Improving container ship panel stress prediction, based on another highly correlated panel stress measurement, Marine Structures", Vol 4, pp. 138–145
Jian, Z., Gaidai, O., Gao, J., 2018, "Bivariate Extreme Value Statistics of Offshore Jacket Support Stresses in Bohai Bay", Journal of Offshore Mechanics and Arctic Engineering, Vol. 140
Kenworthy J et al (2024) "Wind turbine main bearing rating lives as determined by IEC 61400–1 and ISO 281: a critical review and exploratory case study. Wind Energy 27:179. https://doi.org/10.1002/we.2883
Liu Z, Gaidai O, Xing Y, Sun J (2023) Deconvolution approach for floating wind turbines. Energy Sci Engine 11:2742. https://doi.org/10.1002/ese3.1485
Maienza C, Avossa AM, Picozzi V et al (2022) Feasibility analysis for floating offshore wind energy. Int J Life Cycle Assess 27:796–812. https://doi.org/10.1007/s11367-022-02055-89
Manuel L, Veers PS, Winterstein SR (2001) Parametric models for estimating wind turbine fatigue loads for design. J Sol Energy Eng 123(4):346–355
McCluskey CJ, Guers MJ, Conlon SC (2021) Minimum sample size for extreme value statistics of flow-induced response. Marine Struct 79:103048. https://doi.org/10.1016/j.marstruc.2021.103048
Moriarty PJ, Holley WE, Butterfield S (2002) Effect of turbulence variation on extreme loads prediction for wind turbines. J Sol Energy Eng 124(4):387–395
NOAA official website, accessed on May 1st 2023, https://www.ndbc.noaa.gov/station_page.php?station=46041
Peeringa JM (2009) Comparison of extreme load extrapolations using measured and calculated loads of a MW wind turbine. ECN, Petten
Poujol B, Prieur-Vernat A, Dubranna J, Besseau R, Blanc I, Pérez-López P (2020) Site-specific life cycle assessment of a pilot floating offshore wind farm based on suppliers' data and geo-located wind data. J Ind Ecol 24(1):248–262. https://doi.org/10.1111/jiec.1298
Robertson AN, Wendt F, Jonkman JM, Popko W, Dagher H, Gueydon S, Soares CG (2017) OC5 project phase II: validation of global loads of the Deep-C-wind floating semi-submersible wind turbine. Energy Procedia 137:38–57
Ronold KO, Larsen GC (2000) Reliability-based design of wind-turbine rotor blades against failure in ultimate loading. Eng Struct 22(6):565–574
Ronold KO, Wedel-Heinen J, Christensen CJ (1999) Reliability-based fatigue design of wind-turbine rotor blades. Eng Struct 21(12):1101–1114
Sharar, S., Hoover, C., 2024, "Reliability and Preventive Maintenance of Ducted Wind Turbines", https://doi.org/10.48550/arXiv.2403.09760
Stewart GM, Lackner MA, Arwade SR, Hallowell S, Myers AT (2015) Statistical estimation of extreme loads for the design of offshore wind turbines during non-operational conditions. Wind Eng 39(6):629–640
Sun J, Gaidai O, Wang F et al (2023) Gaidai reliability method for fixed offshore structures. J Braz Soc Mech Sci Eng 46:27. https://doi.org/10.1007/s40430-023-04607-x
Sun J, Gaidai O, Xing Y, Wang F, Liu Z (2023) On safe offshore energy exploration in the Gulf of Eilat. Qual Reliabil Engine Int 39:2957. https://doi.org/10.1002/qre.3402
Xu X, Xing Y, Gaidai O, Wang K, Patel K, Dou P, Zhang Z (2022) A novel multi-dimensional reliability approach for floating wind turbines under power production conditions. Front Marine Sci 9:970081. https://doi.org/10.3389/fmars.2022.970081
Yakimov V, Gaidai O, Wang F, Wang K (2023) Arctic naval launch and recovery operations, under ice impact interactions. Appl Engine Sci 15:100146. https://doi.org/10.1016/j.apples.2023.100146
Yakimov V, Gaidai O, Wang F, Xu X, Niu Y, Wang K (2023) Fatigue assessment for FPSO hawsers. Int J Naval Architect Ocean Engine 15:100540. https://doi.org/10.1016/j.ijnaoe.2023.100540
Yuan W, Feng J, Zhang S, Sun L, Cai Y, Yang Z, Sheng S (2023) "Floating wind power in deep-sea area: Life cycle assessment of environmental impacts. Adv Appl Energy 9:100122. https://doi.org/10.1016/j.adapen.2023.100122
Zhang J, Gaidai O, Ji H, Xing Y (2023) Operational reliability study of ice loads acting on cargo vessel bow. Heliyon 9:e15189. https://doi.org/10.1016/j.heliyon.2023.e15189

Publisher's Note